17 March 1966

TRW-9878-6004-R0000

AMBIGUITIES IN THE DATA FROM TILTED, SPINNING FLUXGATE MAGNETOMETERS: APPLICATION TO IMP-1

by

R. W. Fredricks and E. W. Greenstadt

Space Physics Analysis Department
Space Sciences Laboratory
TRW Systems
Redondo Beach, California

and

C. P. Sonett

Space Sciences Division
NASA Ames Research Center
Moffet Field, California

FACILITY FORM 602

X66-36295 (ACCESSION NUMBER)

N67-87199 (THRU)

41 (PAGES)

2A (CODE)

TMX 57413 (NASA CR OR TMX OR AD NUMBER)

30 (CATEGORY)

TRW Systems
One Space Park
Redondo Beach, California

[redacted]

ABSTRACT

Data from a satellite-borne, tilted, spinning fluxgate magnetometer are subject to inherent ambiguities when the sampled ambient field is dynamically active. These ambiguities are further compounded when the sampling is multirate. In this paper, the intrinsic limitations of a multirate-sampled, tilted fluxgate system are described, the production of fictitious ambient vectors is explained, and the conditions for extracting meaningful physical quantities, such as field magnitudes and power spectra, are discussed. The results are applied to the Explorer 18 (IMP-1) magnetometer system in the transition region, and it is shown that the ambiguities of the system do in fact limit the interpretability of the Explorer 18 data there or in any other region of magnetic activity. The impossibility of precisely identifying "collisionless shock" and "turbulent field" phenomena is discussed, and the probable role played by indeterminate errors of the IMP fluxgate system in producing the discrepancies between Explorer 18 magnetometer and other transition zone field and plasma observations is noted.

[redacted]

AMBIGUITIES IN THE DATA FROM TILTED, SPINNING FLUXGATE MAGNETOMETERS: APPLICATION TO IMP-1

by

R. W. Fredricks, E. W. Greenstadt, and C. P. Sonett

1. INTRODUCTION

The most extensive satellite-borne magnetometer measurements to date were made by Explorer 18 (1963-46A, or "IMP-1") in late 1963 and the first half of 1964 (Ness, Scearce, and Seek 1964; Ness, Scearce, Seek, and Wilcox 1965). These measurements, which covered at least part of all the distinct regions surrounding the Earth -- interplanetary space, the magnetosphere, the transition zone, and the geomagnetic tail -- have served both to establish conclusively the permanent existence of these regions and to verify those gross characteristics of each of them previously identified or only conjectured on the basis of sparser evidence from earlier spacecraft or from ground observations. [Rather than encumber this introduction with reference to the extensive literature on both geomagnetic and interplanetary fields, we direct the reader to the bibliography prepared by Hess, Mead, and Nakada (1965).] In addition, certain special features of the physical medium in which the Earth resides have been identified, by interpretations of the Explorer 18 magnetometer record, as a "collisionless shock" separating the solar wind from the transition zone, a "turbulent" or "chaotic" transition zone field (Ness et al. 1964), a neutral surface in the tail (Ness 1965b), a solar-wind sector structure (Wilcox and Ness 1965), and a "magnetohydrodynamic lunar wake" (Ness 1965a, c).

There are, however, discrepancies with earlier work; Sonett, Judge, and Kelso (1959) and Sonett and Abrams (1963) described a preference in transition region fields for certain periodicities there, and Sonett and Abrams (1963) reported 100 gamma field enhancements in the Pioneer I transition zone. Neither phenomenon has been reported in published Explorer 18 results.

More recent publications by several authors have also revealed discrepancies between their results and those of the Explorer 18 magnetometer in the transition region. Wolfe, Silva, and Myers (1966) reported that their locations for the transition zone outer boundary agreed with those of Ness et al. (1964) in approximately 79% of the IMP-1 passes, while their locations of the magnetopause agreed only 64% of the time with those of the magnetometer. Individual examination of the nine transition boundary locations for which graphs of magnetometer data have been published by Ness et al. (1964), Ness (1965a), and Ness et al. (1965) shows that in only two cases did the "shock" positions agree to within .1 earth radius with positions given in Tables 1 and 2 of Wolfe et al. (1966), while in two cases the locations disagreed altogether, in four cases they permitted possible overlap, and in the remaining case only a questionable boundary could be identified from the magnetometer data. Fairfield and Cahill (1966) noted that the 1961 transition zone fields determined by Explorer 12 were in general larger than those of Explorer 18. Heppner (1965) and Holzer, McCleod, and Smith (1966) identified the transition zone boundaries determined by instruments on OGO-1 by abrupt changes of factors of 2 to 4 in dc field magnitude, as well as by the sudden occurrence of field fluctuation, whereas the data of Ness et al. (1964) seemed to show the same magnitude effect only once.

Since it is natural that space physicists should use the Explorer 18 data to look beyond mere identification of significant spatial regions and into the detailed physics of the Earth's environment, it is important to consider the meaning of these discrepancies and to try to isolate instrumental contributions before physical explanations are offered. Such isolation is especially necessary because the Explorer 18 magnetometer data were processed, regardless of the nature of the raw data, on the assumption that the instruments were sampling a constant ambient field. We must therefore consider the potential dynamic behavior of the medium, examining with care the magnetic aspects of this behavior

and the way these may reveal themselves in the data taken with the Explorer 18 magnetometer. In this paper, we present the results of such an examination in which we have studied the capabilities of the instrument and of instruments of comparable design, to provide useful information on the physics of the Earth's distant magnetic environment.

The results are disappointing. We find that sequentially sampled, tilted, spinning fluxgate experiments in general, and the Explorer 18 experiment in particular, are inherently incapable of rendering an accurate picture of the ambient field when that field varies to any appreciable degree and, moreover, that some of the already inferred properties of the distant field, particularly in the transition region, must be accepted with reservations or rejected entirely because of effects based on subtleties in the complex process of data collection, sampling, and reduction. The effects to which we refer seem not to be generally appreciated, although they are well known to communication theorists and magnetometer specialists. These are 1) the difficulty of accounting for spin-signal folding in the raw data (Sonett 1966), 2) the problem of determining signal shapes on the basis of multiply periodic sampling, which introduces compound spectral folding into the processed data and, most importantly, 3) the impossibility of reconstructing three dimensional magnetic vectors from uniaxial or biaxial measurements with tilted fluxgates (Greenstadt 1966, Appendices A and C), a condition we call "vector aliasing".

Spectral folding and vector aliasing occur when certain, rather stringent, conditions on the sampled ambient field are violated. The familiar condition required for accurate scalar signal spectral analysis is that data sampling rates exceed the frequencies present in the ambient signal by at least double the highest frequency component in the signal (the Nyquist frequency); the condition for credible vector reconstruction is that any variation in the ambient field be slow in comparison with the spin rate of the spacecraft. It is the third difficulty mentioned in the preceding paragraph, vector reconstruction, to which this paper is primarily devoted, for other measurements clearly demonstrate violation of the second condition. The first Pioneer I

measurements (Sonett, et al. 1959), for example, revealed the presence of transition zone field oscillations, the details of which were described in several subsequent publications by Sonett and collaborators (see Hess, Mead, and Nakada 1965). Lately, the search coil magnetometers aboard OGO-1 (Holzer et al. 1965) have shown that the magnetic field in the transition region is fluctuating with significant energy over the frequencies encompassed by the bandwidth (0-5 c/s) of the fluxgate magnetometers on Explorer 18. Also, the triaxial fluxgate magnetometer on the same OGO (Heppner 1965) has measured significant sporadic fluctuations of the transition region field at frequencies from about 0.8 c/s to 1.2 c/s, with amplitudes up to several gammas (compared with the apparent dc level of some 10-30 gammas), and, finally, large field oscillations with periodicities 9 to 40 sec are apparent in preliminary observations of the VELA 3 magnetometers (Greenstadt, Inouye, Green, and Judge 1966). This information, coupled with the results of this paper, casts reasonable doubt on the reliability of the vector available from any spinning, tilted fluxgate in the transition region, even with perfect, unsampled data signals, and casts even further doubt on the published quantities derived from the reduction procedure applied to data taken by Explorer 18 in any region of significant magnetic disturbance. These observations may help to explain both the apparent discrepancy between Explorer 18's transition region field magnitudes and those detected by Pioneer I (Sonett and Abrams 1963) and Explorer 12 (Fairfield and Cahill 1966), and the failure of the Explorer 18 experiment to report the multiple boundary crossings observed by OGO-1 (Holzer et al. 1965; Heppner 1965), Mariner 4 (Coleman, Smith, Davis, and Jones 1966), and VELA (preliminary unpublished data).

In Section 2 we discuss the general response of a tilted, spinning fluxgate magnetometer, and specialize to certain types of field fluctuations, showing that unless the ambient field $\underset{\sim}{B}$ is quiet ($\delta \underset{\sim}{B} \ll \underset{\sim}{B}$), or unless the energy spectrum contains components of significance only near zero frequency, the tilted fluxgate magnetometer cannot yield a trustworthy measure of the ambient field. In Section 3 we describe the effects of multirate sampling on a fluxgate signal, showing that in general unambiguous power spectra cannot be obtained when the ambient

field oscillates significantly. In Section 4 we review the data processing employed by the Explorer 18 experiments, showing the dependence of their procedure on assumed field-time independence. In Section 5 we apply the analysis of Sections 2 and 3 to Explorer 18's measurements in the transition region, showing that both the published data of the Explorer 18 magnetometer themselves and the more recent measurements of field fluctuations by OGO-1 and VELA empirically support the conclusion that the theoretical difficulties described in this paper actually do destroy the effectiveness of the magnetometer in this region, or, indeed, of any comparable instrument in any other region of like character.

2. THE OUTPUT OF A SPINNING, TILTED FLUXGATE MAGNETOMETER

In this section we present the general equation for the output of a spinning, tilted fluxgate and then specialize it for two selected types of possible ambient field fluctuation. We shall employ the notation of Ness et al. (1964), in order to permit later application, without change, to the results to Explorer 18.

The two distinct types of ambient field fluctuations we shall consider are, first a purely amplitude modulated field $\underset{\sim}{B}(t) = \underset{\sim}{e}_1 B(t)$, where $\underset{\sim}{e}_1$ is a constant vector, and, second, a purely phase modulated field where the field amplitude is constant, but the direction ψ, in spacecraft coordinates (see Fig. 1), varies. The more general case in which both amplitude and phase modulated fields are present and coupled, while magnetodynamically more realistic, is not treated here, since the two unmixed cases serve as adequate illustrations of the inherent ambiguity in analyzing modulated data. A less specialized treatment of uncoupled amplitude and phase modulated field measurements by both fluxgate and search coils has been presented by Sonett (1966).

General Fluxgate Geometry and Output Signal. The geometry of a typical tilted fluxgate magnetometer is shown in Fig 1. The spacecraft is assumed to spin about the z-axis at the rate ω_m rad/sec. The ambient field vector $\underset{\sim}{B}(t)$ is directed at an angle α to the spin axis, and its projection on the x-y plane normal to the spin axis subtends an angle ψ_o to the projection of the sun-satellite line on the x-axis at t = 0.

The fluxgate axis of sensitivity subtends an angle θ to the spin vector $\underline{\omega}$ (i.e., to the z-axis).

The fluxgate's continuous output signal, generalized to the time dependent case, is written

$$f(t) = B(t)\,[\cos\alpha(t)\,\cos\theta + \sin\alpha(t)\,\sin\theta\,\cos(\omega_m t-\psi(t))] \tag{2-1}$$

or, in terms of ambient field components $B_{||}(t) = B(t)\cos\alpha(t)$ and $B_{\perp}(t) = B(t)\sin\alpha(t)$, respectively parallel and perpendicular to the spin axis,

$$f(t) = B_{||}(t)\,\cos\theta + B_{\perp}(t)\,\sin\theta\,\cos[\omega_m t-\psi(t)]. \tag{2-2}$$

In later sections, we shall also need the first and second time derivatives of f. These are given, in terms of $B_{\perp}$ and $B_{||}$, by

$$\dot{f}(t) = -B_{\perp}(t)\sin\theta[\omega_m-\dot{\psi}(t)]\sin[\omega_m t-\psi(t)]+B_{\perp}\sin\theta\cos[\omega_m t-\psi(t)] +\dot{B}_{||}(t)\cos\theta \tag{2-3}$$

and

$$\begin{aligned}\ddot{f}(t) = {} & B_{\perp}(t)\sin\theta\left\{\ddot{\psi}(t)\sin[\omega_m t-\psi(t)]\cos[\omega_m t-\psi(t)]\right\} \\ & -2\dot{B}_{\perp}(t)\sin\theta[\omega_m-\dot{\psi}(t)]\sin[\omega_m t-\psi(t)] \\ & +\ddot{B}_{\perp}(t)\sin\theta\cos[\omega_m t-\psi(t)]+\ddot{B}_{||}(t)\cos\theta\ .\end{aligned} \tag{2-4}$$

We note at once the complexity of these expressions in contrast to the simplified contractions which result when vector $\underline{B}$ is (or as with Explorer 18, is assumed) constant (see Section 4). The resulting simplifications [Eqs. 4-1, 2, 3], although superficially advantageous in terms of permitting a simple straightforward algebraic solution for the basic parameters of the dc component of ambient field, pay an obvious penalty in inaccuracy when the neglected terms are significant and can be used with confidence only in regions known in advance, or inferred on strong evidence, to be magnetically quiet.

Amplitude Modulated Field. We now specialize to the case of an ambient field of constant direction, but varying amplitude, given by

$$B(t) = B_o + \sum_{n=1}^{N} B_n \cos(n\Omega t - \varphi_n). \tag{2-5}$$

By suitable choice of Ω, φ_n, B_n, and N such a Fourier series can approximate any reasonable waveform B(t) over a restricted time interval $0 \le t \le T$.

If (2-5) is combined with (2-1) the resulting output function is

$$\begin{aligned} f(t) = {} & B_o A_o + B_o A_1 \cos(\omega_m t - \psi) + \sum_{n=1}^{N} B_n A_o \cos(n\Omega t - \varphi_n) \\ & + (1/2) \sum_{n=1}^{N} B_n A_1 \Big\{ \cos[(\omega_m + n\Omega)t - (\psi + \varphi_n)] \\ & + \cos[(\omega_m - n\Omega)t - (\psi - \varphi_n)] \Big\}, \end{aligned} \tag{2-6}$$

where $A_o = \cos\alpha \cos\theta$, $A_1 = \sin\alpha \sin\theta$. The first and second derivatives of f are

$$\begin{aligned} \dot{f}(t) = {} & \omega_m B_o A_1 \sin(\omega_m t - \psi) + \sum_{n=1}^{N} n\Omega B_n A_o \sin(n\Omega t - \varphi_n) \\ & + (1/2) \sum_{n=1}^{N} B_n A_1 \Big\{ (\omega_m + n\Omega) \sin[\omega_m + n\Omega)t - (\psi + \varphi_n)] \\ & + (\omega_m - n\Omega) \sin[\omega_m - n\Omega)t - (\psi - \varphi_n)] \Big\}, \end{aligned} \tag{2-7}$$

and

$$\begin{aligned} \ddot{f}(t) = {} & \omega_m^2 B_o A_1 \cos(\omega_m t - \psi) + \sum_{n=1}^{N} n^2\Omega^2 B_n A_o \cos(n\Omega t - \varphi_n) \\ & + (1/2) \sum_{n=1}^{N} B_n A_1 \Big\{ (\omega_m + n\Omega)^2 \cos[\omega_m + n\Omega)t - (\psi + \varphi_n)] \\ & + (\omega_m - n\Omega)^2 \cos[(\omega_m - n\Omega)t - (\psi - \varphi_n)] \Big\}. \end{aligned} \tag{2-8}$$

In a magnetic survey experiment, the unknown field parameters of such a field are B_n and φ_n, and it is obvious that many higher derivatives than the first two shown above are required to supply enough equations for solution. Since, in a practical data reduction procedure, the differentials would be obtained by nth order differences, it follows that for large N, rather long records are needed if the Nth difference is to be based on enough points to carry significance. If only the dc component of the ambient field is desired, it can be obtained, provided $\Omega \not\approx \omega_m$, by passing the raw signal from the instrument through a narrow pass-band filter centered at ω_m. Of course if the ambient energy contained in the dc component is only a minor fraction of the total field energy, the result is of little interest. The specific application of this type of limitation to Explorer 18 data in the transition region will be given in Section 5, but we illustrate the potential difficulty here with an elementary example:

Most researchers who have processed sequentially sampled data are familiar with the term "aliasing", which describes the overlapping of spectral orders centered on harmonics of the sampling frequency, i.e., the situation in which the sum of a sampling frequency harmonic and the frequency of one signal component is equal to the sum of another sampling frequency harmonic and the frequency of second signal component. Under this circumstance, the separate contributions cannot be distinguished. As the main point of this paper, we call attention to an analagous phenomenon peculiar to the tilted spinning fluxgate, which we designate "vector aliasing" to describe a situation where nonconstant frequency components of the ambient field can simulate false vector projections in the spacecraft frame. This phenomenon is not to be confused with the more obvious difficulty which occurs when the three components of a variable vector are sampled sequentially over a time period comparable to that with which the vector changes. As a simple, elegant example of vector aliasing, let $\Omega = \omega_m$, $\alpha = 0$, $B_o = 0$, and $N = 1$ in Eq. (2-6). Then

$$f(t) = B_1 \cos\theta \cos(\omega_m t - \varphi_1) ,$$

according to which a signal produced by a variable field along the satellite spin axis is identical in every way to, and indistinguishable from, the signal which would be produced by a constant field of magnitude $B_\perp$ perpendicular to the spin axis. Note that in cases of this kind, no accumulation of equations or narrow pass filters and no wide band telemetry, no matter how perfect, can help distinguish the true from the false vector. A second distinct example of vector aliasing caused by the second chosen type of modulation is discussed next.

Phase Modulated Field. The second special case we use for illustration is one in which the amplitude B and polar angel α of the ambient field are constant, while the azimuthal angle $\psi(t)$ is a linear function of time. We have, from (2-1), and its first and second derivatives,

$$f(t) = B\left\{A_o + A_1 \cos\left[\omega_m t - \psi(t)\right]\right\}, \tag{2-9}$$

$$\dot{f}(t) = -(\omega_m - \dot{\psi})BA_1 \sin\left[\omega_m t - \psi(t)\right] \tag{2-10}$$

$$\ddot{f} = -(\omega_m - \dot{\psi})^2 BA_1 \cos\left[\omega_m t - \psi H)\right] + \ddot{\psi} BA_1 \sin\left[\omega_m t - \psi(t)\right], \tag{2-11}$$

where A_o and A_1 are defined as before.

If $\psi(t) = \Omega t + \varphi$, then

$$f(t) = B\left\{A_o + A_1 \cos\left[(\omega_m - \Omega)t + \varphi\right]\right\}, \tag{2-12}$$

$$\dot{f}(t) = -(\omega_m - \Omega)BA_1 \sin\left[(\omega_m - \Omega)t + \varphi\right], \tag{2-13}$$

and

$$\ddot{f}(t) = -(\omega_m - \Omega)^2 BA_1 \cos\left[(\omega_m - \Omega)t + \varphi\right]. \tag{2-14}$$

In the nearly synchronous case, $\omega_m \approx \Omega$, the instrument will appear to yield a constant output signal

$$f(t) = B(A_o + A_1 \cos\varphi). \tag{2-15}$$

This case, because of the apparent absence of spin modulation, could be erroneously interpreted as a static ambient field directed along the spin axis, when actually the ambient field is rotating, with constant amplitude, in synchronism with the spacecraft's rotation. The apparent ambient 'vector' deduced in this situation could even be orthogonal to the true one if, say, $\alpha = \pi/2$, and thus entirely false.

Before applying these generalities and hypothetical cases to the Explorer 18 experiment, we look briefly in the next section at the additional, more conventional ambiguities arising when any signal is subjected to multirate sampling.

3. MULTIRATE SAMPLING LIMITATIONS ON SPECTRAL ANALYSIS

Often, when absolute or relative magnitudes cannot be found reliably from experimental data, much useful information still may be gained by examining the frequencies present when recorded signals fluctuate. We therefore discuss briefly the problem of extracting scalar averages such as power spectral density from fluctuating fields seen by a tilted fluxgate system and subjected to multiply periodic sampling of the particular form used by Explorer 18.

We begin with a general expression g(t) for the train of data pulses from a single fluxgate in terms of the continuous fluxgate signal f(t). As before, we employ a notation directly applicable to the Explorer 18 special case. We write

$$g(t) - f(t)\, u_1\,(t,\tau,T_s)u_2(t,T_1,T_2)\ , \qquad (3\text{-}1)$$

where u_j is the unit sampling function and the parameters τ, T_s, T_1, and T_2 correspond to characteristic parameters of the Explorer 18 data format shown partially in Fig. 2, and explained fully in the next section. The expansion of (3-1) explicitly in its Fourier representation is

$$g(t) = f(t)\left\{\tau/T_s + 2\tau/T_s \sum_{n=1}^{N} \frac{\sin(n\pi\tau/T_s)}{n\pi\tau/T_s} \cos n\omega_s(t-\tau/2)\right\}$$

$$\cdot\left\{T_1/T_2 + 2T_1/T_2 \sum \frac{\sin(m\pi T_1/T_2)}{m\pi T_1/T_2} \cos m\omega_2(t-T_1/2)\right\} \qquad (3\text{-}2)$$

where $\omega_s = 2\pi/T_2$.

The frequency spectrum of (3-1) is given by

$$G(\omega) = \int_{-\infty}^{\infty} f(t)u_1(t,\tau,T_s)u_2(t_1T_1,T_2)e^{i\omega t}dt$$

which can be expressed as the double convolution integral

$$G(\omega) = \int_{-\infty}^{\infty} d\omega'' \int_{-\infty}^{\infty} d\omega' \; F(\omega-\omega')U_1(\omega'-\omega'',\tau,T_s)U_2(\omega'',T_1,T_2) \qquad (3\text{-}3)$$

where

$$F(\Omega) = \int_{-\infty}^{\infty} f(t)e^{i\,\Omega\,t}dt$$

$$U_1(\Omega,\tau,T_s) = \int_{-\infty}^{\infty} u_1(t)e^{i\,\Omega\,t}dt = \tau/T_s\left\{\delta(\Omega)\right.$$

$$\left. + \sum_{n=1}^{\infty} \frac{\sin(n\pi\tau/T_s)}{n\pi\tau/T_s}\left[e^{-in\omega_s\tau/2}\delta(\Omega+n\omega_s) + e^{in\omega_s\tau/2}\delta(\Omega-n\omega_s)\right]\right\}$$

$$U_2(\Omega,T_1,T_2) = \int_{-\infty}^{\infty} u_2(t)e^{i\,\Omega\,t}dt = T_1/T_2\left\{\delta(\Omega)\right.$$

$$\left. + \sum_{m=1}^{\infty} \frac{\sin(m\pi T_1/T_2}{m\pi T_1/T_2}\left[e^{-im\omega_2T_1/2}\delta(\Omega+n\omega_2) + e^{im\omega_2T_1/2}\delta(\Omega-n\omega_2)\right]\right\}.$$

One can write (3-3) in the explicit form

$$G(\omega) = xyF(\omega) + xy\sum_{n=1}^{\infty} \frac{\sin n\pi x}{n\pi x}\left[e^{-in\pi x}F(\omega+n\omega_s)+e^{+in\pi x}F(\omega-n\omega_s)\right]$$

$$+ xy\sum_{m=1}^{\infty} \frac{\sin m\pi y}{m\pi y}\left[e^{-im\pi y}F(\omega+m\omega_2)+e^{im\pi y}F(\omega-m\omega_2)\right]$$

$$+\sum_{n=1}^{\infty}\sum_{m=1}^{\infty} \frac{\sin n\pi x \sin m\pi y}{nm\pi^2 xy}\left[e^{-i\pi(nx+my)}F(\omega+m\omega_2+n\omega_s)\right.$$

$$+ e^{i\pi(nx-my)}F(\omega+m\omega_2-n\omega_s)$$

$$\left. + e^{-i\pi(nx-my)}F(\omega-m\omega_2+n\omega_s) + e^{i\pi(nx+my)}F(\omega-m\omega_2-n\omega_s)\right] , \quad (3\text{-}4)$$

where $x \equiv \tau/T_s$, $y = T_1/T_2$, and the spectrum $F(\omega)$ is given by

$$F(\omega) = \int_{-\infty}^{\infty} e^{i\omega t}f(t)dt = \int_{-\infty}^{\infty} B(t)\left[A_o+A_1\cos(\omega_m t-\psi)\right]e^{i\omega t}d\omega$$

and $A_o = \cos\alpha\cos\theta$, $A_1 = \sin\alpha\sin\theta$.

The amplitude spectrum of the unsampled signal is formally

$$F(\omega) = A_o b(\omega) + (1/2)A_1\left\{e^{-i\psi}b(\omega+\omega_m) + e^{i\psi}b(\omega-\omega_m)\right\} , \quad (3\text{-}5)$$

and $b(\omega)$ is the amplitude spectrum of the ambient field amplitude

$$b(\omega) = \int_{-\infty}^{\infty} e^{i\omega t}B(t)dt .$$

We note from equations (3-4) and (3-5) the following important limitations on the ability to extract the power spectrum of the ambient field. The power spectrum of the sampled signal can be expressed as

$$P_g(\omega) = G(\omega)G^*(\omega) = |G^2(\omega)| \ , \tag{3-6}$$

where $G^*(\omega)$ is the complex conjugate of $G(\omega)$. We see from (3-4) that the product (3-6) will contain terms of the type

$$\begin{aligned} F(\omega)F^*(\omega) = {} & A_o^2|b(\omega)|^2 + \frac{A_1^2}{4}\left\{|b(\omega+\omega_m)|^2 + |b(\omega-\omega_m)|^2\right\} \\ & + e^{-i\psi}\left\{b^*(\omega)b(\omega+\omega_m)+b(\omega)b^*(\omega-\omega_m)\right\} \\ & + e^{i\psi}\left\{b^*(8)b(\omega-\omega_m)+b(\omega)b^*(\omega+\omega_m)\right\} \\ & + e^{i2\psi}b(\omega-\omega_m)b^*(\omega+\omega_m) + e^{-i2\psi}b^*(\omega-\omega_m)b(\omega+\omega_m), \end{aligned} \tag{3-7}$$

and it is obvious that the leading term (3-7) of the product (3-6) will represent the unaliased power spectrum $|b^2(\omega)|$ of the ambient field only if the cross products $b(\omega)b^*(\omega\pm\omega_m)$ etc. all vanish. This is a condition on the bandwidth of $b(\omega)$ and the spin frequency ω_m. The term (3-7) would be the only contributor to the product (3-6) if there were no sampling, i.e., if there were continuous telemetry transmission of the fluxgate signal f(t). It follows from (3-7) that <u>unless the spectrum $b(\omega)$ vanishes for $\omega > \omega_m/2$ the power spectrum of the ambient field cannot be extracted from the data even in the absence of sampling</u>.

However, in the presence of the multirate sampling expressed by equation (3-4), the limitation just given for the continuous signal case is not even applicable. When $\omega_m \gg (\omega_s,\omega_2)$ there occur in the product (3-6) terms of the sort

$$\frac{\sin\pi x}{\pi x} F(\omega)F^*(\omega+n\omega_s) \quad n = 1,2,3 \ \ldots$$

$$\frac{\sin m\pi y}{m\pi y} F(\omega)F^*(\omega+m\omega_2) \quad m = 1,2,3 \ \ldots$$

which in turn imply products of the form

$$\frac{\sin n\pi x}{n\pi x}\, b(\omega) b^*(\omega \pm n\omega_s) \tag{3-8a}$$

$$\frac{\sin m\pi y}{m\pi y}\, b(\omega) b^*(\omega \pm m\omega_2) \tag{3-8b}$$

If $\omega_2 < \omega_s$, the overlapping spectral products (3-8b) will place a more severe limitation on the bandwidth of $b(\omega)$ required to avoid an aliased power spectrum. It will be shown in Section 4 that just these conditions prevail in the case of the Explorer 18 magnetometer.

4. THE EXPLORER 18 MAGNETOMETER SYSTEM

In this section, we review those aspects of the Explorer 18 system necessary to this paper. For a more complete description of the magnetometers and data sampling procedure the reader is referred to the report of Ness et al. (1964).

The Satellite Data System. Explorer 18's fluxgates, denoted as 'A' and 'B', were mounted on booms 180° apart, with fluxgate A tilted at $\theta_A = 60°$ and B at $\theta_B = 30°$ relative to $\underset{\sim}{\omega}$. The telemetry sampled the continuous signal f(t) for an interval of 4.8 sec each 20.5 sec in the sequence: A-B-A-B.....-A-B, for a total of 12 samples (six from fluxgate A, alternating with six from fluxgate B). A 102 second gap in this sampling then occurred during which the rubidium vapor magnetometer was read out, and the entire sequence was then repeated.

The sampling format is shown schematically in Figure 2. If the A and B sensors are treated as an equivalent single instrument by correcting for the difference in tilt angle and for any existing relative offset fields of the two sensors, this sampling is multirate, consisting of 12 samples of 4.8 sec duration separated by 20.5 sec gaps (a total of $T_1 = 225.5$ sec), followed by an unsampled gap of 102.5 sec, and having an overall (12 sample set) repetition period of $T_2 = 328$ sec. (Our times are rounded-off approximations to the exact times given by Ness et al.) Thus, the fluxgate data recorded on the ground were in the form of analog (amplitude modulated) pulses of 4.8 sec duration in the sequence

just described. The first, approximately 0.8 sec portion of each pulse contained an impressed calibration signal. These leading portions of each pulse were therefore excluded from the data analysis (Ness, private communication) thus reducing the effective length of each pulse to $\tau = 4.0$ sec.

On the ground, each 4.8 sec analog pulse was digitized at intervals of 0.16 sec. Of the 30 digital points so derived, the first five were discarded to eliminate the calibration signal, as previously discussed. The remaining 25 points were scanned by a suitable prediction filter to eliminate the obviously 'bad' points due to telemetry drop-out or other artificial sources (Ness, private communication). If more than 10 percent of the digital points in any given sample were inconsistent with the predictor program, the entire sample was omitted in computing an average field $\overline{B}_m$.

Subsequent to the data scan just described, acceptable samples containing the nominal number of 25 digital points were numerically filtered to extract the first harmonic and the first and second time derivatives of the digitized signal at the nominal spin frequency. The numerical filters were presumably narrow banded.

Data Reduction Equations. The magnetometer data reduction method was based not on the general equations (2-2, 3, and 4); but, rather, on their contractions for constant field approximation:

$$f(t) = B_{\parallel} \cos\theta + B_{\perp} \sin\theta \cos(\omega_m t - \psi), \tag{4-1}$$

$$\dot{f}(t) \simeq -\omega_m B_{\perp} \sin\theta \sin(\omega_m t - \psi), \tag{4-2}$$

and

$$\ddot{f}(t) \simeq -\omega_m^2 B_{\perp} \sin\theta \cos(\omega_m t - \psi) . \tag{4-3}$$

Clearly, (4-1, 2, and 3) can be consistent with (2-2, 3, and 4) only if the variations represented by $\dot{B}_{\|}(t)$, $\ddot{B}_{\|}(t)$, $\dot{B}_{\perp}(t)$, $\ddot{B}_{\perp}(t)$, $\dot{\psi}(t)$, and $\dot{\alpha}(t)$ are all negligible on the scale of the variation $\cos \omega_m t$. However, if these differential coefficients of the sinusoids of argument $\omega_m t$ vary or are otherwise non-negligible, as one could expect in locally disturbed magnetic fields, the entire data reduction procedure based on constant $\underset{\sim}{B}$ becomes invalid, for the most part, in an indeterminate way.

If the time variable terms above <u>are</u> in fact negligible, the desired vector quantities $B_{\|}$, $B_{\perp}$, α, and ψ can be found from the equations

$$\omega_m t_o - \psi = \arctan\left[\omega_m \dot{f}(t_o)/\ddot{f}(t_o)\right] , \tag{4-4}$$

$$\omega_m^4 B_{\perp}^2 \sin^2\theta = \omega_m^2 \dot{f}^2(t_o) + \ddot{f}^2(t_o) , \tag{4-5}$$

$$B_{\|}\cos\theta = f(t_o) - B_{\perp}\sin\theta\cos(\omega_m t_o - \psi) , \tag{4-6}$$

and

$$\alpha = \arctan\left[B_{\perp}(t_o)/B_{\|}(t_o)\right] , \tag{4-7}$$

where the instant $t = t_o$ can be selected in a convenient way. This instant was chosen by the Explorer 18 experimenters (Ness, private communication) to correspond to the central point of the 25 digital points used in analyzing one sample. The above expressions (4-4) - (4-7) are those used in reducing the Explorer 18 data. The vector computed from (4-4) - (4-7) was transformed to the solar ecliptic coordinate frame (x, y, z) and the components in that frame were averaged over each nominal 12 sample sequence to produce a 5.46 min averaged vector $\bar{\underset{\sim}{B}}$ of components

$$\bar{B}_j = N^{-1} \sum_{n=1}^{N} B_j(n) \quad . \tag{4-8}$$

Variances

$$\overline{\delta B_j^2} = N^{-1} \sum_{n=1}^{N} \left[\overline{B}_j - B_u(n) \right]^2 \tag{4-9}$$

and standard deviations $(\overline{\delta B_j^2})^{1/2}$, called variances by Ness et al., were also computed for the 12 samples. In the remainder of this paper we shall use the terms variance and standard deviation interchangeably.

Certain broad statements about built-in ambiguities in the Explorer 18 system can be made at once. The data reduction procedure was designed to extract numerically only the dc and spin frequency components of the sensor signal, and was in no way intended to find other frequencies or to compute nth derivatives of the magnetometer output. At best, therefore, only the unvarying portion of the ambient field vector could be obtained, no matter how insignificant this fraction of the total field vector might be. Consider, however, the amplitude modulated illustration of eqs. (2-6, 7, 8), where ambient fluctuations at the spin frequency ($\Omega=\omega_m$) appear as dc and second harmonic terms. Since the Explorer 18 spin rate varied over the first 70 days of flight from $f_m = 0.371$ cps to $f_m = 0.405$ cps, it follows that in regions of space where the ambient field spectrum b(f) contained significant energy in frequencies in the range 0.371 to 0.405 cps, no useful quantitative information of any kind, vector properties or r.m.s. amplitude, could possibly be extracted from the specified fluxgate data reduction procedure because of spin modulation-field fluctuation heterodyning.

Furthermore, inherent aliasing of the power spectrum was shown in Section 3 [Eq. (3-8)] to occur if the ambient field spectrum $b(\omega)$ contains significant energy at frequencies $\omega > 1/2\ \omega_2 = \pi/T_2$. For Explorer 18 (see Fig. 2), $T_2 = 328$ sec. Thus the ambient spectrum must not contain energy at frequencies $f > 0.0015$ cps if power spectra are to be computed, since the amplitude factor $(\sin \pi y)/\pi y$ in Eq. (3-8) is $(\sin 56^\circ)/2.16 = 0.38$ which is not small compared with unity. It follows that for the sampling format of Explorer 18's fluxgates, the applicable Nyquist frequency is $f_n = 0.0015$ cps.

5. MEASUREMENTS BY EXPLORER 18 IN THE TRANSITION REGION

So far, we have shown that a tilted, spinning fluxgate magnetometer is subject generally to inherent ambiguities arising when the ambient field in which the sensor rotates is dynamically active. We have also shown what happens to the signal from such an instrument when certain hypothetical examples of ambient field behavior are present, and we have shown the additional complications which may arise when the sensor output is subjected to a particular type of multirate sampling. Finally, we have shown that the Explorer 18 magnetometer system was a multirate-sampled, tilted, spinning fluxgate system potentially open to all the ambiguities of such systems in the presence of magnetodynamic activity along the trajectory of the vehicle. In this section we demonstrate that the limitations imposed on tilted fluxgate experiments by a magnetodynamic medium actually affected the Explorer 18 instrument in the transition region. We then discuss the bearing these ambiguities have on physical inferences drawn from the Explorer 18 results.

Significance of the 5.46 min Variances. The first indication that sections of the Explorer 18 data are affected by the ambiguities outlined in this paper occurs in the published graphs of the vector quantities derived from the data themselves. The figures contained, for example, in the preliminary report of Ness *et al.* (1964) and in a later report on the "lunar wake" by Ness (1965a) clearly show that the variances (4-9) are non-zero over substantial portions of the satellite orbit. In fact, Ness *et al.* (1964) characterized the transition region and, partially, the lunar wake, by the continuous presence of non-zero standard deviations, i.e., by the existence of field fluctuations for which $\frac{\delta \overline{B}}{B}$ was appreciable (0.5 - 2.0). But, it is in just such cases of large proportional deviations $\delta\overline{B}/\overline{B}$ that it may be impossible to extract unambiguous vector properties of the ambient field from the fluxgate data. The existence of a given 5.46 (actually 3.7) min, non-zero standard deviation means that during the interval giving rise to the deviation, the sampled field contained periodicities shorter than 225 sec.

Fluctuations of periods less than 225 sec could create a variance in either of two ways: first, periods of, say, 10 to 225 sec, would give differing fields for each of the 12 samples used in computing the variance; second, periods between 20 sec and the magnetometer filter cutoff of .2 sec, would tend to distort the individual evaluations of $B_{\parallel}$ and $B_{\perp}$, giving rise to quantities artificially aliased in the vector sense, and in no way required to be consistent from one sample to the next. Existence of the second source of variance in the transition zone is established by the appearance of degenerate spin-modulated waveforms in Explorer 18's raw data (Ness et al. 1965). Thus, we may conclude tentatively that the magnitudes and directions of the transition region fields published by Ness et al. could be significantly in error, and that vector quantities corresponding to sections of the published graphs within which the 5.46 min standard deviations are non-zero could be fictitious constructions fabricated by the automated data reduction scheme.

We next ask just what quantitative errors might have been induced by field variation, and to do so we turn to some later measurements with other types of systems in the transition region.

Effect on the Explorer 18 Experiment of Oscillations Observed by OGO-1. A preliminary report by Heppner (1965) on the OGO-1 fluxgate magnetometers, which transmitted their information at a much higher bit rate than did those of Explorer 18, has shown the existence near the transition zone boundary of field oscillations in the range 0.8 to 1.2 cps, with amplitudes comparable to the background field magnitude. In the notation of Section 2 of this report, we suppose the oscillations were of the form (2-5), with $\Omega/2\pi \approx 2(\omega_m/2\pi)$, and $B_1 \approx B_o$. Then a narrow (ideal) filter centered on ω_m would pass the following portions of (2-6, 7, 8):

$$f(t) = B_o A_1 \cos(\omega_m t - \psi) + (1/2) B_1 A_1 \cos(\omega_m t + \psi - \varphi_1) \tag{5-1}$$

$$\dot{f}(t) = \omega_m B_o A_1 \sin(\omega_m t - \psi) + (1/2) B_1 A_1 \omega_m \sin(\omega_m t + \psi - \varphi_1) \tag{5-2}$$

$$\ddot{f}(t) = \omega_m^2 B_o A_1 \cos(\omega_m t - \psi) + (1/2) B_1 A_1 \omega_m^2 \cos(\omega_m t + \psi - \varphi_1) \tag{5-3}$$

where we have set $n = 1$ and $\Omega = 2\omega_m$. According to Eq. (4-4) the apparent spacecraft-field coordinate ψ' is computed from

$$\omega_m t_o - \psi' = \arctan\left\{\frac{B_o \sin(\omega_m t_o - \psi) + (1/2)B_1 \sin(\omega_m t_o + \psi - \varphi_1)}{B_o \cos(\omega_m t_o - \psi) + (1/2)B_1 \cos(\omega_m t_o + \psi - \varphi_1)}\right\} \tag{5-4}$$

Equation (3-8) leads to the identity $\psi' \equiv \psi$ only under two very special conditions: The first is obviously that of the perfectly quiet field $B_1 = 0$, or its approximation $B_1 \ll B_o$; and second is that $2\psi = \varphi_1$, which also gives $\psi' = \psi$. The latter is a condition on the relative phases of the ambient field and the vector component in the spin plane but this cannot be assumed to hold always for any arbitrary time of measurement. A reasonable assumption would be uncorrelated angles ψ and φ_1.

It follows that for $B_1 \sim B_o$ and an arbitrary relationship between φ_1 and ψ, the expression (5-4) will yield an angle ψ' which differs from the true angle ψ. Also, this spurious angle ψ' depends upon the instant of time, $t = t_o$, chosen to evaluate (5-4). It also depends, for fixed $t = t_o$, on the phase $\psi - \varphi_1$ and the relative amplitudes B_o and B_1.

To demonstrate the risk of computing ψ' from (4-4) when (5-4) is valid, we note that if $R = R_1/B_o$, then

$$\omega_m t_o - \psi' = 0 \text{ when } 2\sin(\omega_m t_o - \psi) = -R\sin(\omega_m t_o + \psi - \varphi_1)$$

$$\omega_m t_o - \psi' = \pi/2 \text{ when } \left[\cos(\omega_m t_o - \psi) + (1/2)R\cos(\omega_m t_o + \psi - \varphi_1)\right] \to 0^+$$

$$\omega_m t_o - \psi' = -\pi/2 \text{ when } \left[\cos(\omega_m t_o - \psi) + (1/2)R\cos(\omega_m t_o + \psi - \varphi_1)\right] \to 0^-$$

and it follows that the angle ψ' can be in error by $\pm 90^\circ$ depending upon R, ψ, φ_1, and t_o.

The qualitative behavior of ψ' is elucidated by considering the functions

$$N(\omega_m t_o - \psi, \varphi_1, R) = \sin(\omega_m t_o - \psi) + (R/2)\sin(\omega_m t_o - \psi + \delta)$$

$$D(\omega_m t_o - \psi, \varphi_1, R) = \cos(\omega_m t_o - \psi) + (R/2)\cos(\omega_m t - \psi + \delta),$$

where $\delta \equiv 2\psi - \varphi_1$. For $R \ll 1$, the zeros of $N(\omega_m t_o - \psi, \varphi_1, R)$ and $D(\omega_m t_o - \psi, \varphi_1, r)$ cannot differ radically from those of $\sin(\omega_m t_o - \psi)$ for phase shifts $-\pi < \delta < \pi$. Hence, under these conditions the error $|\psi' - \psi|$ will be small. The maximum possible error $|\psi' - \psi|$ in computed value of azimuthal angle <u>versus</u> the ratio $R = B_1/B_o$ is shown in Table 1. Note that the OGO-1 measurements (Heppner 1965) indicate ratios $0 < R \approx 1$.

Table 1. Maximum Error $|\psi' - \psi|$ for Various $R = B_1/B_o$

R	0	0.25	0.50	0.75	1.0	2.0	>> 2
$\lvert\psi' - \psi\rvert$	0°	7°	12°	19°	30°	45°	90°

To determine possible errors in amplitude, consider Eq. (4-5) which presumably defines $B_\perp = B \sin \alpha$. From (4-5), (5-2), and (5-3) the <u>apparent</u> field component $B'_\perp$ is given by

$$(B'_\perp)^2 = (B_{o\perp})^2 \left\{1 + R^2/4 + R \cos \delta \right\},$$

$$B_{o\perp} = B_o \cos \alpha$$

$$\delta = 2\psi - \varphi_1 . \qquad (5\text{-}5)$$

The limiting errors for fixed $R = B_1/B_o$ occur for $\delta = 0$ and $\delta = \pi$:

$$\left.\begin{aligned} B'_\perp/B_{o\perp} &= (1+R+R^2/4)^{1/2} \quad (\delta=0) \\ B'_\perp/B_{o\perp} &= (1-R+R^2/4)^{1/2} \quad (\delta=\pi) \end{aligned}\right\} \qquad (5\text{-}6)$$

We emphasize that $B_{o\perp}$ is the very low frequency component of the true ambient field perpendicular to the spin axis, and is the contribution most important in forming a 5.46 minute average as described in Section 4. The minimum and maximum values of the ratio $B'_{\perp}/B_{o\perp}$ of apparent-to-true low frequency components are shown in Table 2 as a function of $R = B_{\perp}/B_{o}$.

Table 2. Minimum and Maximum Values of $B'_{\perp}/B_{o\perp}$ for Increasing R

$R = B_{\perp}/B_{o}$	0	0.25	0.50	0.75	1.0	2.0	$\gg 2$
$B'_{\perp}/B_{o\perp}, (\delta=\pi)$	1.000	0.875	0.750	0.625	0.500	0.000	∞
$B'_{\perp}/B_{o\perp}, (\delta=0)$	1.000	1.125	1.250	1.375	1.500	2.000	∞

Similar calculations can be carried out to ascertain the discrepancy between the apparent field component $B'_{\parallel}$ and polar angle α', and the true ambient values $B_{o\parallel}$ and α. However, the above results are adequate to illustrate the possible ambiguities or erroneous vectors which can result from an indiscriminate application of the quiet field approximations (4-1, 2, 3) to a case in which the ambient field is amplitude modulated in a coherent fashion. In general, the Fourier transform of the ambient field fluctuations will be a continuum, and there is a clear risk of passing through a filter centered on $\omega = \omega_m$ energy which is shifted from some frequency band $\Delta\ (n\,\Omega)$ in the inertial frame of the ambient field into the passband of the filter by means of spin modulation-amplitude modulation heterodyning.

The calculations of the foregoing paragraphs demonstrate quantitatively the kinds of errors to which individual vector parameters contributing to Explorer 18's 5.46 min, 12 pt averages were subject in the presence of field behavior known to exist in parts of the transition region. Of course, we have used the particular assumption that the ambient oscillations were entirely attributable to an amplitude-modulated field, whereas, in general, one should expect coupled longitudinal and

transverse waves and irregular pulsations of any polarization. Nevertheless, we see that the "vectors" computed from Explorer 18 data under the assumption of constant ambient field are in error by indeterminate amounts in the transition region, and, without independent evidence to the contrary, may be equally ambiguous wherever $\dot{\underset{\sim}{B}} \not\approx 0$.

Averaged Vectors from Fluctuating Fields. As the preceding calculations show, individual values of the apparent vector quantities $|\underset{\sim}{B}'|$, α', and ψ' computed from a sample of the tilted fluxgate signal f(t) by applications of (4-4) - (4-7) can be significantly in error. The averages calculated using (4-8) involve the arithmetic means of (nominally) twelve such values. If these individual values can have significant errors, then in general the arithmetic averages formed from them will be erroneous. The reader can easily verify that the r.m.s. deviations computed from (4-8) will be significantly different from zero for many varieties of field spectra. Indeed, one can easily prove that the r.m.s. deviations will be appreciable if either (1) the ambient field is "turbulent", "chaotic", or "noisy" (in any well defined sense of such terminology), or (2) the ambient field possesses coherent oscillations as treated above and in Section 2. There is no unambiguous way to determine which sort of fluctuating field is responsible for the r.m.s. deviation simply by looking at this quantity alone. Moreover, since $B'_{\parallel}$, $B'_{\perp}$, and ψ were transformed to field components in the cartesian SEC frame before computation of 12-sample averages and variances, errors in either would be distributed among all three cartesian components, making them all subject to the errors of the spacecraft measurement system.

Based on the results of this study, one can indeed use the r.m.s. deviations published for the Explorer 18 experiment as a gauge of the degree of confidence one may assign to the field "vectors" given at corresponding times. It seems clear from our calculations that whenever the r.m.s. deviation $\langle \delta B^2 \rangle^{1/2}$ is comparable to (i.e., same order of magnitude as) the averaged field amplitude $\langle B^2 \rangle^{1/2}$, the ambient field was too disturbed for equations (2-5, 6, 7) to be valid, and the "vector" quantities $\langle B' \rangle$, $\langle \psi' \rangle$ and $\langle \alpha' \rangle$ (or their solar ecliptic equivalents) need not bear any close relationship to the true values $\langle B \rangle$, $\langle \psi \rangle$, and $\langle \alpha \rangle$ of the very low frequency constituent of $\underset{\sim}{B}(t)$.

Twelve Point Averages of Transition Zone Data Seen by VELA Magnetometers. To illustrate the relationship between Explorer 18's 12-point (5.46 min) averages and transition region fields, we examine a data sample obtained with one of the third launch VELA magnetometers. These instruments are search coils measuring the ambient field projection $B_\perp$ on the plane normal to the VELA spin axes, along with the angle ψ on the same plane, between the field projection and the sun-spin axis plane. The $B_\perp$ component is measured through a low pass filter with cutoff at 0.1 cps; the vehicle spins at approximately 2 cps, and the telemetry sampling rate for $B_\perp$ is one pt every 2 seconds, so that the Nyquist frequency is .25 cps. The instruments themselves are subject to conventional aliasing by ambient signals at twice the spin rate and to small spurious contributions arising from the differentiating nature of the sensor (Sonett 1963), but, of course, they are completely insensitive to vector aliasing.

In Fig. 3 is a section of the VELA record showing a sample of transition region field close to the dawn meridian at 18 R_e and 274° solar ecliptic longitude. The upper graph is a machine plot of the raw data representing the magnitude of $B_\perp$. The lower curve is a smoothed version of the upper graph, formed by the three point running mean of the raw data. Underneath the two curves is displayed the 5.46 min sampling format of Explorer 18; the curves themselves have been drawn alternately solid and dashed to reflect this format, the solid segments representing portions of the data that might have been sampled by the Explorer 18 system.

The field oscillations depicted in Fig. 3 are especially large in amplitude, but, in character, not untypical of VELA transition region data examined up to the time of writing. The plotted data are from the "coarse" readings of the VELA System, with approximately 6 γ digitization. Both fine readings and the phase measurements ψ corresponding to the section of data in the figure show considerable fluctuation. We call attention to the comparative coherence of the measured component over intervals on the order of minutes; to the resemblance between the data periodicities and those of certain common types of pc and pt micropulsations observed in geomagnetic ground records; and to the apparent 12

to 20 γ amplitudes on the measurement plane of these large transition region waves. The amplitudes are comparable to the total transition field values reported near the shock by Heppner (1965) and are roughly 50 to 100% of the field magnitudes shown by Fairfield and Cahill (1966). At the same time, the amplitudes are as much as double the total "vector" magnitude typically seen by Explorer 18 in the transition zone (Ness et al. 1964).

The superposed Explorer 18 data format serves to demonstrate the difficulties of interpreting the 5.46 min averages. The average of the first group of twelve samples in Fig. 3 would be close to the mean of the signal which could, for the sake of example, be 5 γ, implying a small dc contribution to $B_\perp$. The corresponding standard deviation would be non-zero, in this case, because of the presence of coherent, quasi-sinusoidal oscillations rather than "disordered" fields. The dc and variance values would form a poor representation of the ambient field's comparatively organized distribution of energy.

The peak to peak periods in the smoothed sample of Fig. 4 tend to be near 12, 24, or 36 seconds. We may easily imagine a field sample of similar pattern, but with 20.5 second period, during which chance might place 12 samples 20.5 sec apart, in phase with the signal zero-crossings, so that even the standard deviations would be negligible, regardless of the fluctuation amplitude.

Finally, we note that on the shorter 4-sec time scale of each sample, $B_\perp$ is changing enough in some cases to distort the looked-for spin modulated signal. During the sixth 4-sec sample (from the left) of Fig. 4, for example, $B_\perp$ varies by some 10 to 12 γ. The asymmetric spin-waveform created by such a short-term change would lead to a dc contribution interpreted falsely as a part of $B_\parallel$. Moreover, since this fictitious part of $B_\parallel$ would vary from sample to sample, the 12-sample average of $B_\parallel$ would in turn have a non-zero standard deviation even though the true $B_\parallel$ were perfectly constant.

We see, therefore, the way in which inaccuracy and ambiguity can be created in the Explorer 18 data by the relationship between the combination of magnetometer and telemetry format and the kinds of fields known to be in the transition region.

Physical Inferences. We are finally in a position to ask what may be the physical implications of Explorer 18's inability to monitor accurately the magnetic field in regions of magnetodynamic activity. The answer is fairly simple. Because of the inherent limitations on the Explorer 18 fluxgate experiment caused by vector aliasing, and the imposed limitations of spin modulation and sampling format, neither the vector nor the scalar (r.m.s.) field in very disturbed parts of the transition region can be deduced with confidence by any means from the available data. In particular, details of the physics of the transition region's shock-like outer boundary, or even the location of the boundary, cannot become known accurately on the basis of these magnetometer measurements.

The only safe interpretation of Explorer 18's emergence from a region of large $\overline{\delta B}/\overline{B}$ to one in which this parameter is small is very crude: it moves from a region of significant but unknown fluctuations in the local field $\underset{\sim}{B}(t)$ to one of reasonably steady field $\underset{\sim}{B}_0$ of measurable properties. Without more detailed information than this, confirmation of any theory of a shock transition between the geomagnetosphere and the solar wind by the Explorer 18 experiment cannot be made, even if we were to accept the problematical hypothesis that magnetometer data by themselves, uncorrelated with plasma measurements, can verify or contradict collisionless shock theory. The OGO-1 data, for example (Heppner 1965), show the existence of nearly coherent, ~ 1 cps, field oscillations exactly at the apparent boundary between the solar wind and the transition zone, and trailing off on either side of the interface. The boundary, in this case, was identified by an apparent sudden change in the background field itself, rather than by the presence or absence of fluctuation, and the same criterion of sudden change in dc field was mentioned by Holzer et al. (1966), although a simultaneous fluctuation boundary was also noted. The Explorer 18 instrument would respond differently to the ambient fields on either side of this boundary, but in neither case would it necessarily provide a correct measurement of even the dc component. Moreover, we can but speculate on the reaction of the Explorer 18 system to the multiple boundary crossings reported by Holzer et al. (1965), Coleman et al. (1966), and evident in preliminary VELA 3 data now being analyzed by the TRW magnetometer group.

The ambiguity of even locating the shock on the basis of the 5.46 min variance criterion is evident on examination of just the few published graphs of processed magnetometer data covering the shock crossing. The difficulty in defining objectively a precise terminus or onset of significant variances can be seen, for example, in Figures 14, 17, 19, 21, 33 of Ness et al. (1964), where sudden changes in variance may (Fig. 19) or may not (Fig. 33) correspond to simultaneous abrupt changes in the constructed dc field vector; where variances sometimes fade out gradually to low, but non-zero, levels; and where jumps in variance occur in what is apparently interplanetary space. The annoyance of having to use the tilted fluxgate data and their standard deviations to identify collisionless shock locations was clearly recognized by the Explorer 18 experimenters, for on orbit 6 inbound (Fig. 21 of Ness et al. 1964) they were forced to abandon the customary variance criterion altogether in an effort to define a "questionable" shock from discontinuities in the constructed vector components alone, at a point several earth radii distant from either of two "shock" locations given by Wolfe et al. (1966) for the same pass, and where nothing of interest affected the variances.

The converse, of course, should not be overlooked in the face of these rather negative results of our evaluation of the Explorer 18 experiment. Wherever (1) $\overline{\delta B}/\overline{B}$ is small, as evidenced by negligible 5.46 min standard deviations, and the computed field vector is relatively steady with time or, (2) in the absence of deviations, where the vector seems to form a particularly steady, coherent, and repeatable pattern, we may feel secure in concluding that the constructed vectors are very close to the true ambient magnetic field. These conditions apply to most of the published interplanetary data and to the measurements by Explorer 18 in the Earth's magnetic tail (Ness et al. 1965) although the absence of variance graphs in figures accompanying the tail data leaves in doubt some sections where the computed vectors are apparently less ordered than usual, especially in view of Anderson's (1965) observations of rapid fluctuation in energetic electron population.

Finally, we note that the limitations we have discussed in this paper apply anywhere outside the transition region when $\overline{\delta B}/\overline{B}$ is appreciable, a condition probably evidenced by the appearance of non-zero 5.46 min standard deviations. The ambiguities caused by vector aliasing

would therefore apply to the processed vectors and their deviations during the period of 14-15 December 1963 in which Explorer 18 is alleged to have encountered the Moon's magnetohydrodynamic wake (Ness 1965a, c). Since virtually any kind of field fluctuation -- sinusoidal or disordered-- could produce, in the tilted fluxgate, output signals giving rise to non-zero standard deviations and artificial vectors, the suggested identification of the lunar wake by virtue of the "similarity" of the mid-December variances to those observed habitually by Explorer 18 in the Earth's transition region (Ness 1965c) would be unjustified even if no alternative explanation of the fluctuating field behavior were available (Greenstadt 1965; Hirshberg 1966).

6. CONCLUSIONS

We have investigated the data processing problem presented by a multirate sampled, spin-modulated, tilted fluxgate magnetometer signal, with particular attention to the transition region results of the Explorer 18 magnetometer experiment. The results of the investigation have led to the following conclusions:

1) The vector properties of the ambient magnetic field deduced from tilted fluxgate data using the procedure described in Section 4 are reliable when the r.m.s. deviation $(\overline{\delta B^2})^{1/2} \ll \overline{B}$. Thus, the majority of the published <u>interplanetary</u> magnetic field measurements deduced from Explorer 18 magnetometer data by assuming $B \approx 0$ appear to be valid.

2) The vector properties of the ambient field deduced from tilted fluxgate data by using the method of Section 4 are quantitatively erroneous when the r.m.s. deviation $(\overline{\delta B^2})^{1/2} \approx \overline{B}$. Thus, the published <u>transition region</u> magnetic field measurements of Explorer 18 are probably unreliable and may bear no obvious relationship to the ambient field vector. The same statement applies to the measurements during <u>disturbed periods</u> in the interplanetary medium, such as the "lunar wake", or the magnetosphere. Furthermore, the assignment of "chaos" to the transition region field on the basis of large variances is unjustified since coherent field oscillations also can produce such

variances, and the "shock" locations defined generally on the basis of variance onset cannot be unambiguously and objectively delineated.

3) Because of multirate sampling of the Explorer 18 fluxgate signals, no reliable (unaliased) power spectrum $|b^2(\omega)|$ of the ambient magnetic field (and thus no r.m.s. field magnitude) can be deduced from the sampled data if the ambient field contains significant energy in fluctuations at frequencies $f > 0.0015$ c/s, which is the lowest Nyquist frequency associated with the data sampling format. Since $(\overline{\delta B^2})^{1/2} \approx \overline{B}$ implies significant fluctuations at frequencies $f > 0.0044$ cps, it is clear that all of the Explorer 18 transition region data are intrinsically aliased.

4) In view of the foregoing, the assertions that Explorer 18 data provided "continuous vector monitoring" of the magnetic field, and that "...accurate measurements of the vector magnetic field by the IMP-1 experiment ... permit the investigation separately of directional changes and magnitude changes" (Ness, 1965c) cannot be taken seriously for portions of the orbit within the transition region and for segments of any orbit in interplanetary space or the magnetosphere along which the r.m.s. deviations are a reasonable fraction of the averaged field $\overline{B}$.

5) Discrepancies between transition zone results of the Explorer 18 magnetometer and those of other instruments on the same or different spacecraft cannot be resolved on the basis of physical arguments alone.

6) Physical understanding of the solar wind-geomagnetosphere transition zone and of disturbed interplanetary conditions, insofar as such understanding may depend on knowledge of the dynamics of the magnetic field, will have to await the full results of a magnetometer experiment making instantaneous, spin-demodulated, or unmodulated, tri-axial measurements using a wide band telemetry system.

ACKNOWLEDGMENTS

One of us (E.W.G.) wishes to thank his VELA co-experimenters, headed by Dr. G. T. Inouye, and including Dr. I. M. Green and Dr. D. L. Judge, for permission to show some of the VELA date in advance of regular publication; and two of us (R.W.F. and E.W.G.) gratefully acknowledge the support of this work under the TRW Systems Independent Research Program. We enjoyed many stimulating discussions of this work with Dr. F. L. Scarf.

REFERENCES

Anderson, K.A., Energetic Electron Fluxes in the Tail of the Geomagnetic Field, J. Geophys. Res. 70, 4741-4763, 1965.

Coleman, P.J., Jr., E.J. Smith, L.Davis, Jr., and D.E. Jones, Measurements of Magnetic Fields in the Vicinity of the Magnetosphere and in Interplanetary Space - Preliminary Results from Mariner 4, Sixth International Space Science Symposium of COSPAR, Mar del Plata, Argentina, 17 May 1965, Space Research VI, to be published 1966.

Fairfield, D.H., and L.J. Cahill, Jr., Transition Region Magnetic Field and Polar Magnetic Disturbances, J. Geophys. Res., 71, 155-169, 1966.

Greenstadt, E.W., Final Estimate of the Interplanetary Magnetic Field at 1 A.U. from Measurements Made by Pioneer 5 in March and April 1960, Ap.J., in press, July 1966.

Greenstadt, E.W., Interplanetary Magnetic Effects of Solar Flares: Explorer 18 and Pioneer 5, J. Geophys. Res. 70, 5451-5452, 1965.

Greenstadt, E.W., G.T. Inouye, I.M. Green, and D.L. Judge, Observations of Magnetic Pulsation-Like Phenomena at 19 R_e in the Solar Wind-Geomagnetosphere Transition Region, Paper to be presented at 47th Annual Meeting of the AGU, Washington, D.C., April 1966.

Heppner, J.P., Recent Measurement of the Magnetic Field in the Outer Magnetosphere and Boundary Regions, NASA Report No.X-612-65-490, Goddard Space Flight Center, Greenbelt, Maryland, November 1965.

Hess, W.N., G.D. Mead, and M.P. Nakada, Bibliography of Particles and Field Research, Report X-640-65-37, NASA Goddard Space Flight Center, Jan. 1965.

Hirshberg, J., On the Observation of the Moon's Wake, J. Geophys. Res., 71, in press, 1966.

Holzer, R.E., M.G. McLeod, and E.J. Smith, Preliminary Results from the OGO-1 Search Coil Magnetometer: Boundary Positions and Magnetic Noise Spectrums, J. Geophys. Res., 71, 1481-1486, 1966.

Ness, N.F., The Magnetohydrodynamic Wake of the Moon, J. Geophys. Res. 70, 517-534, 1965 a.

Ness, N.F., The Earth's Magnetic Tail, J. Geophys. Res. 70, 2989-3006, 1965 b.

Ness, N.F., Remarks on Paper by E.W. Greenstadt, J. Geophys. Res. 70, 5453-5454, 1965 c.

REFERENCES (Cont'd.)

Ness, N. F., C. S. Scearce, and J. B. Seek, Initial Results of the IMP-1 Magnetic Field Experiment, J. Geophys. Res., 69, 3531-3569, 1964.

Ness, N. F., C. S. Scearce, J. B. Seek, and J. M. Wilcox, A Summary of Results from the IMP-1 Magnetic Field Experiment, Report X-612-65-180, NASA Goddard Space Flight Center, May 1965.

Sonett, C. P., The Distant Geomagnetic Field 2. Modulation of a Spinning Coil EMF by Magnetic Signals, J. Geophys. Res., 68, 1229-1232, 1963.

Sonett, C. P., Modulation and Sampling of Hydromagnetic Radiation, Sixth International Space Science Symposium of COSPAR, Mar del Plata, Argentina, 17 May 1965, Space Research VI, to be published, 1966.

Sonett, C. P. and I. J. Abrams, The Distant Geomagnetic Field 3. Disorder and Shocks in the Magnetopause, J. Geophys. Res., 68, 1233-1263, 1963.

Sonett, C. P., D. L. Judge, and J. M. Kelso, Evidence Concerning Instabilities of the Distant Geomagnetic Field: Pioneer I, J. Geophys. Res., 69, 941-943, 1959.

Wilcox, J. M. and N. F. Ness, Quasi-Stationary Corotating Structure in the Interplanetary Medium, J. Geophys. Res., 70, 5793-5805, 1965.

Wolfe, J. H., R. W. Silva, and M. A. Myers, Observations of the Solar Wind During the Flight of IMP-1, J. Geophys. Res., 71, 1319-1340, 1966.

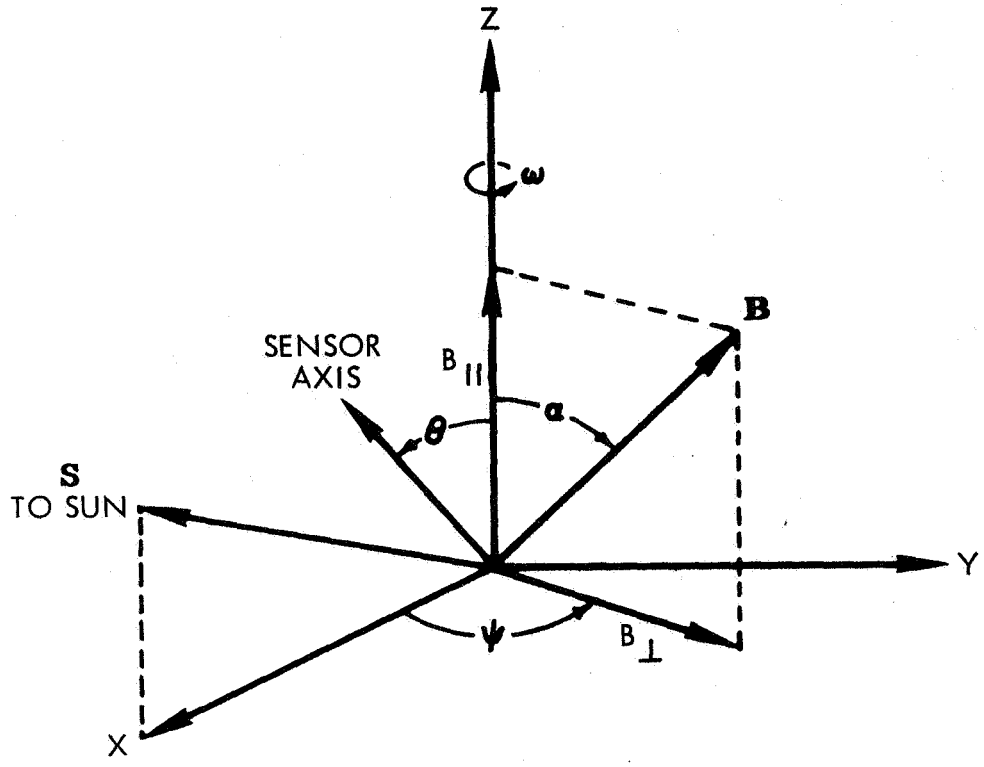

Figure 1. Fixed Spacecraft Coordinate Frame for a Spinning, Tilted Fluxgate System. $\underset{\sim}{B}$ is the ambient field vector, spin vector $\underset{\sim}{\omega}$ is along the z axis, and sun vector $\underset{\sim}{s}$ is in the x-z plane.

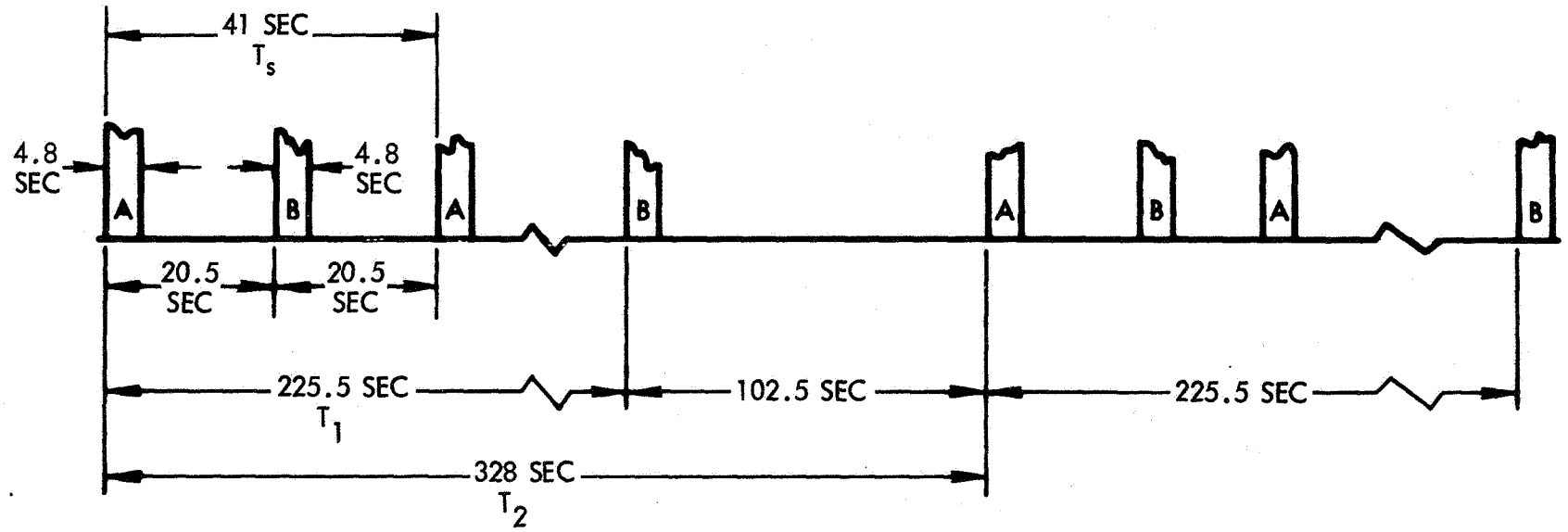

Figure 2. Multirate Sampling Telemetry Format for Explorer 18 Magnetometer.

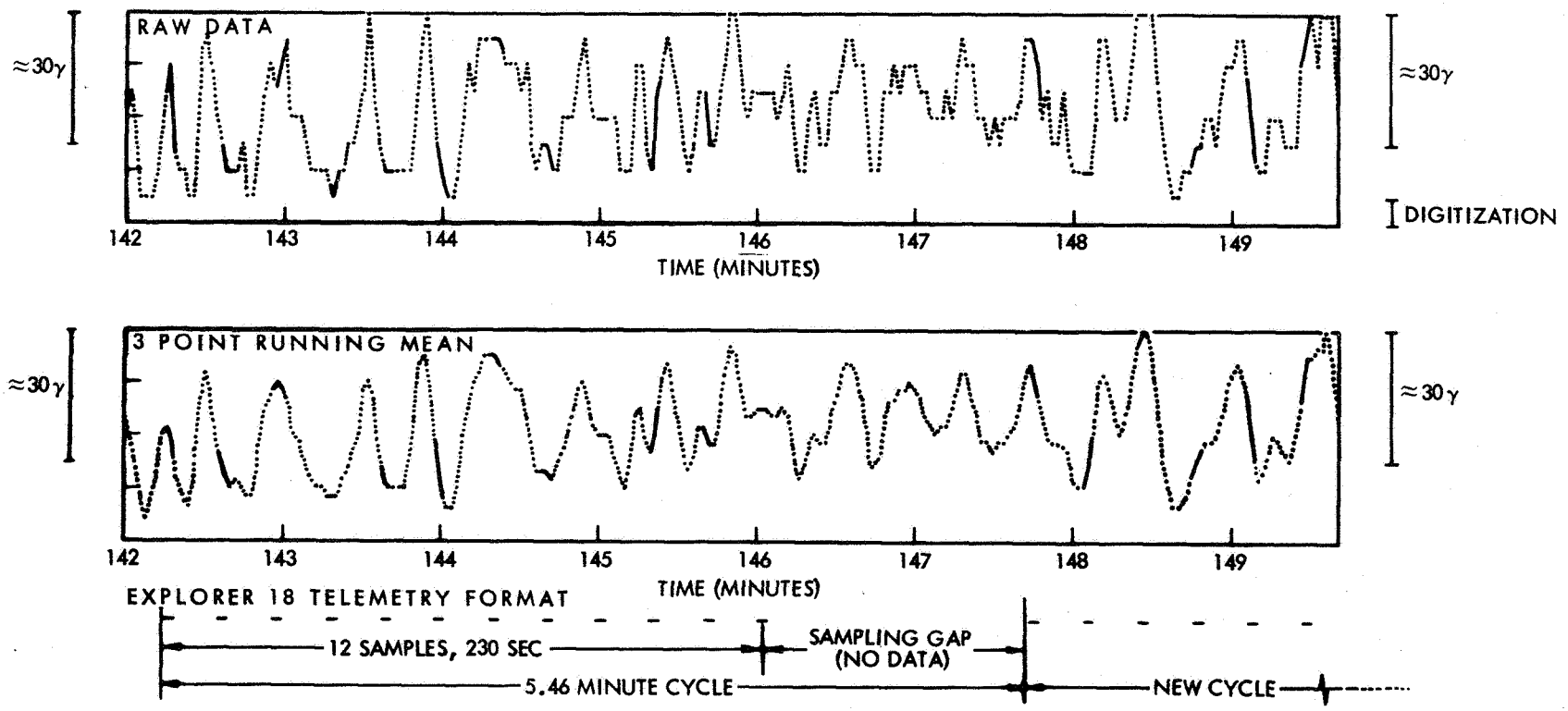

Figure 3. Example of VELA Search Coil Magnetometer Data in the Transition Region, Showing Superimposed Explorer 18 Telemetry Format. Top curve, raw data; center curve, 3 pt. running mean of raw data; bottom, Explorer 18 magnetometer sample timing. Solid segments of data curves represent hypothetical $B_\perp$ data samples which might have been selected by Explorer 18.